

## Stratification of Risk of Progression to Colectomy in Ulcerative Colitis using Measured and Predicted Gene Expression

**Angela Mo<sup>1</sup>§, Sini Nagpal<sup>1</sup>§, Kyle Gettler<sup>2</sup>, Talin Haritunians<sup>3</sup>, Mamta Giri<sup>2</sup>, Yael Haberman<sup>4,5</sup>, Rebekah Karns<sup>4</sup>, Jarod Prince<sup>6</sup>, Dalia Arafat<sup>1</sup>, Nai-Yun Hsu<sup>2</sup>, Ling-Shiang Chuang<sup>2</sup>, Carmen Argmann<sup>7</sup>, Andrew Kasarskis<sup>7</sup>, Mayte Suarez-Farinas<sup>7</sup>, Nathan Gotman<sup>8</sup>, Emebet Mengesha<sup>3</sup>, Suresh Venkateswaran<sup>6</sup>, Paul A. Rufo<sup>9</sup>, Susan S. Baker<sup>10</sup>, Cary G. Sauer<sup>6</sup>, James Markowitz<sup>11</sup>, Marian D. Pfefferkorn<sup>12</sup>, Joel R. Rosh<sup>13</sup>, Brendan M. Boyle<sup>14</sup>, David R. Mack<sup>15</sup>, Robert N. Baldassano<sup>16</sup>, Sapana Shah<sup>17</sup>, Neal S. LeLeiko<sup>18</sup>, Melvin B. Heyman<sup>19</sup>, Anne M. Griffiths<sup>20</sup>, Ashish S. Patel<sup>21</sup>, Joshua D. Noe<sup>22</sup>, Sonia Davis Thomas<sup>23</sup>, Bruce J. Aronow<sup>4</sup>, Thomas D. Walters<sup>20</sup>, Dermot P. B. McGovern<sup>3</sup>, Jeffrey S. Hyams<sup>24</sup>, Subra Kugathasan<sup>6</sup>, Judy H. Cho<sup>2</sup>, Lee A. Denson<sup>4</sup>, Greg Gibson<sup>1\*</sup>**

**A full list of affiliations appears at the end of the manuscript**

§ These authors contributed equally

**\* Corresponding author:**

Greg Gibson, School of Biological Sciences, Georgia Institute of Technology, Atlanta GA 30332

Email: [greg.gibson@biology.gatech.edu](mailto:greg.gibson@biology.gatech.edu) Phone: +1 (404) 385-2343

1      **SUMMARY**

2      **An important goal of clinical genomics is to be able to estimate the risk of adverse disease**  
3      **outcomes. Between 5% and 10% of ulcerative colitis (UC) patients require colectomy**  
4      **within five years of diagnosis, but polygenic risk scores (PRS) utilizing findings from**  
5      **GWAS are unable to provide meaningful prediction of this adverse status. By contrast, in**  
6      **Crohn's disease, gene expression profiling of GWAS-significant genes does provide some**  
7      **stratification of risk of progression to complicated disease in the form of a Transcriptional**  
8      **Risk Score (TRS). Here we demonstrate that both measured (TRS) and polygenic**  
9      **predicted gene expression (PPTRS) identify UC patients at 5-fold elevated risk of**  
10     **colectomy with data from the PROTECT clinical trial and UK Biobank population cohort**  
11     **studies, independently replicated in an NIDDK-IBDGC dataset. Prediction of gene**  
12     **expression from relatively small transcriptome datasets can thus be used in conjunction**  
13     **with transcriptome-wide association studies to stratify risk of disease complications.**

## 14 INTRODUCTION

15        Genetic risk assessment in humans has to date focused mainly on prediction of disease onset  
16    (1), whereas arguably the greater clinical need is for prediction of disease progression (2,3).  
17    Polygenic risk scores (PRS) may sometimes meet both needs, such as the ability of a PRS for  
18    coronary artery disease to stratify people with respect to the likely effectiveness of statins or PCSK9  
19    inhibitors (4-6). This is not generally expected to be the case, however, and in the context of  
20    inflammatory bowel disease, there appears to be little influence of the heritability for disease on  
21    progression to complicated disease (7). Since genome-wide association studies sufficiently powered  
22    to develop accurate PRS for progression or therapeutic response are not yet available, there is a need  
23    for alternative genomic strategies.

24        A promising approach is gene expression profiling, which very often discriminates cases and  
25    controls. For both Crohn's disease and ulcerative colitis, RNAseq of ileal and rectal biopsies  
26    respectively, generates discriminators of disease severity and progression to complications or  
27    remission that are at least as good as clinical indices (8-10). Combining eQTL with GWAS signals  
28    with RNAseq data also supports transcriptional risk scores (TRS), namely weighted sums of  
29    polarized z-scores of transcript abundance, that predict stricturing or penetrating Crohn's disease  
30    (11). As profiling moves to the single cell level, it is clear that gene expression will also define the  
31    identities of critical cell types in which pathogenic alleles act (12-14) and likely refine transcript-  
32    based risk assessment. The main limitation of this approach is the ability to obtain appropriate tissue  
33    biopsies.

34        Consequently, transcriptome-wide association studies (TWAS) have been proposed to fill this  
35    gap (15,16). These are analyses that essentially sum the cis-eQTL effects at a locus in order to  
36    predict gene expression in a case-control cohort where only genotypes are available. Differential

37 expression predictions have been shown to highlight candidate genes for a range of disease (17).  
38 Here we demonstrate that the further utility of TWAS to generate a predicted polygenic  
39 transcriptional risk score (PP-TRS) for ulcerative colitis, which not only discriminates cases, but also  
40 progression to major disease complication requiring colectomy for up to 10% of patients (18-20).  
41 Genomic analysis of just hundreds of individuals, projected onto the UK Biobank (21), supports  
42 polygenic risk assessment that outperforms the current PRS for ulcerative colitis. Our analyses also  
43 provide insight into the cell-type specificity in both epithelial and immune compartments for IBD-  
44 GWAS loci.

45

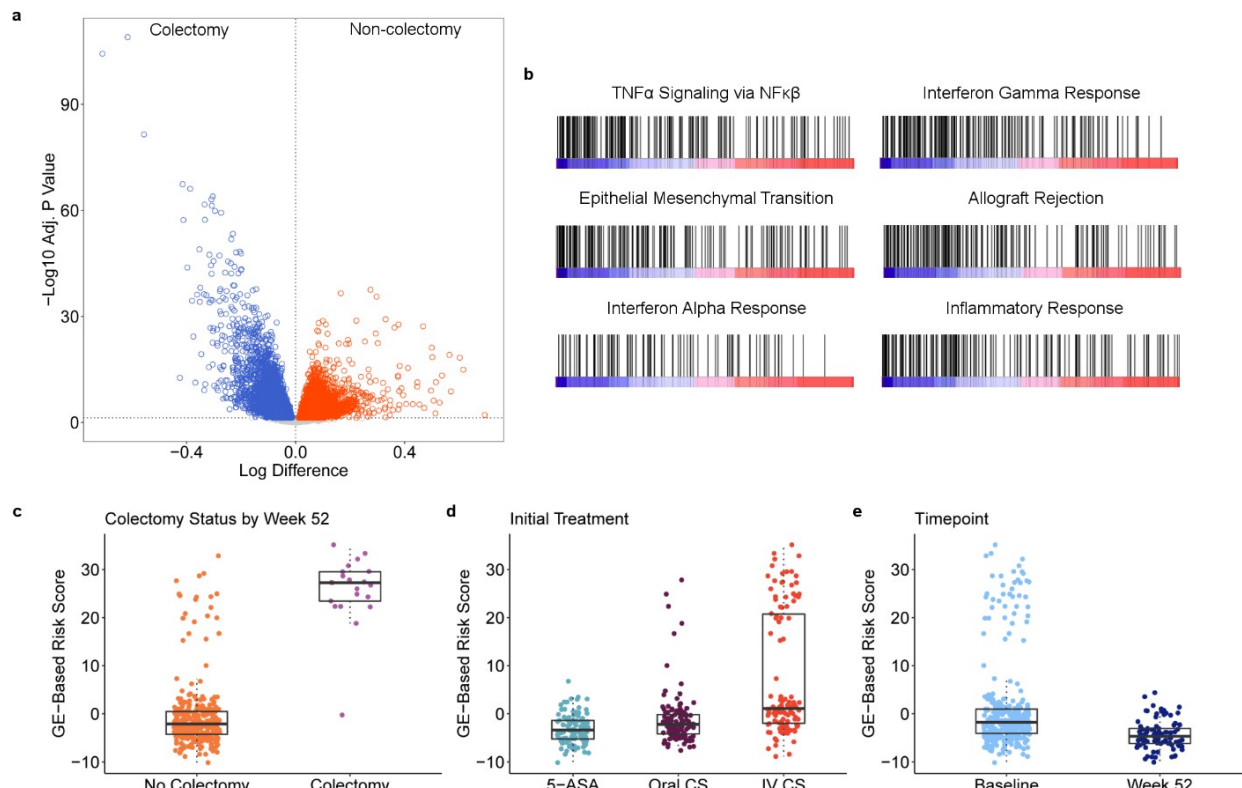
## 46 RESULTS AND DISCUSSION

47 PROTECT is a multicenter pediatric inception cohort study of response to standardized  
48 colitis therapy<sup>9a</sup>. We have previously shown that a signature of rectal mucosal gene expression  
49 at diagnosis, prior to therapeutic intervention, associates with corticosteroid-free remission with  
50 mesalamine alone observed in 38% of 400 patients by week 52 of follow-up<sup>9</sup>. A signature of  
51 rectal mucosal gene expression associated with week 4 corticosteroid response in PROTECT is  
52 related to one indicative of response to anti-TNF $\alpha$  and anti- $\alpha_4\beta_7$  integrin therapy in adults<sup>10</sup>, and  
53 reciprocally, active pediatric UC was associated with suppression of mitochondrial gene  
54 expression, and increasing disease severity with elevated innate immune function. In order to  
55 more explicitly model progression to colectomy observed in 6% (25 of 400) of the patients  
56 within one year of diagnosis, we performed differential expression analysis between baseline  
57 rectal RNAseq biopsies of 21 patients who progressed to colectomy, and 310 who did not. The  
58 volcano plot in Fig. 1a shows down-regulation of 783 transcripts in the colectomy cases (red),  
59 and up-regulation of 1,405 transcripts (blue) at the experiment-wide threshold of  $p < 4 \times 10^{-6}$ .  
60 Gene set enrichment analysis<sup>22</sup> summarized in Fig. 1b highlights engagement of multiple

61 pathways previously implicated in adverse outcomes in inflammatory bowel disease, including  
62 TNF and interferon signaling, and various signatures of inflammation and immune response<sup>8,23</sup>.

63 The first principal component (PC1<sub>col</sub>) of the top 150 of these differentially expressed  
64 genes has a weak negative correlation with our previously reported signature of remission  
65 detected in a subset of 206 patients using a different RNAseq protocol<sup>10</sup>. With very high  
66 significance, it distinguishes the colectomy cases from non-progressors, as all but one case have  
67 PC1 scores greater than 10, a value exceeded by only 20 of the 317 non-colectomy cases (Fig.  
68 1c). This PC1<sub>col</sub> predictor is orders of magnitude more significant than observed with similar  
69 scores derived by 1000 permutations of the data (Fig. S1). All of the high PC1<sub>col</sub> individuals  
70 were placed initially on corticosteroids, the majority intravenously (Fig. 1d); the score also  
71 correlates with a gradient of disease severity indicated by baseline PUCAI (pediatric ulcerative  
72 colitis activity index)<sup>24</sup> and initial treatment. We also obtained rectal biopsy RNAseq data for  
73 92 patients at week 52 and observed significant depression of the score (Fig. 1e), indicative of  
74 mucosal healing even in the cases with elevated initial gene activity (none of the follow-up

75



76

77

78 **Figure 1.** Differential Expression Associated with Colectomy in the PROTECT study. (a) Volcano plot of  
79 significance (negative log10 of the p-value) against difference in expression on log2 scale, with genes  
80 up-regulated in colectomy in blue. (b) Six pathways highlighted by gene set enrichment analysis as up-  
81 regulated in colectomy. Each bar represents a gene in the indicated pathway, and position along the  
82 axis is representative of rank order of differential expression. From left to right, top to bottom, FDR <  
83  $10^{-4}$ ,  $< 10^{-4}$ ,  $< 10^{-4}$ ,  $< 10^{-4}$ ,  $2.4 \times 10^{-4}$ , and  $2.0 \times 10^{-4}$ . A full list of pathways can be found in Table S2. PC1 of  
84 the differentially expressed genes as a function of (c) colectomy status at week 52;  $p = 2 \times 10^{-45}$ , (d) initial  
85 treatment;  $p = 5 \times 10^{-20}$ , and (e) baseline or week 52 follow-up biopsy profile;  $p = 2 \times 10^{-7}$ . All boxplots  
86 indicate 1<sup>st</sup> and 3<sup>rd</sup> quartile as box ends, with center median line and whiskers extending to farthest  
87 point within 1.5 times the interquartile range.

88

89 cases were colectomy, since the surgical procedure had been performed earlier than week 52).

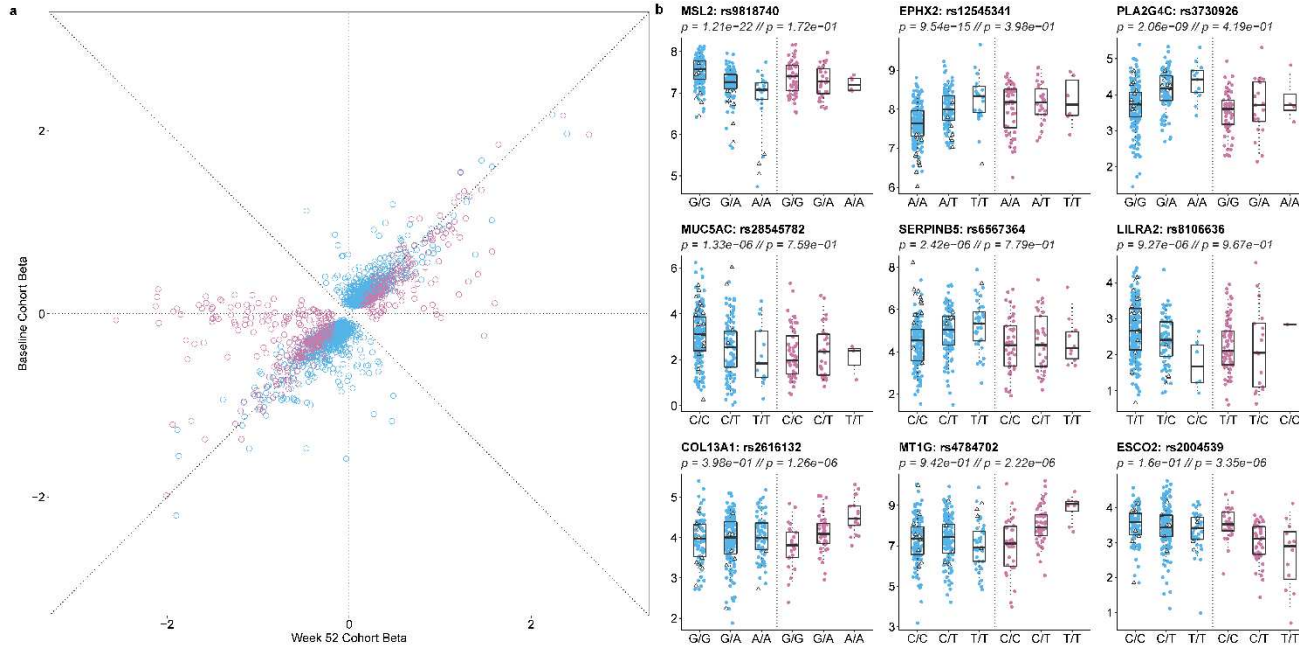
90 Figure S2 shows that PC1 remains associated with Mayo endoscopic score (25) even at week

91 52, and that the change in PC1 molecular score over time correlates with the degree of mucosal

92 healing.

93 Given the marked shift in gene expression at follow-up, we next asked whether local  
94 regulation of the gene expression might contribute, by performing comparative eQTL analysis.

95 Figure 2a indicates generally high concordance in the effect sizes (betas) at both time-points,  
96 with slight inflation of the estimates at baseline (1,416 blue effects) or week 52 (421 magenta  
97 effects), likely due to winner's curse. There were 72 eSNPs significantly regulating 308 genes at



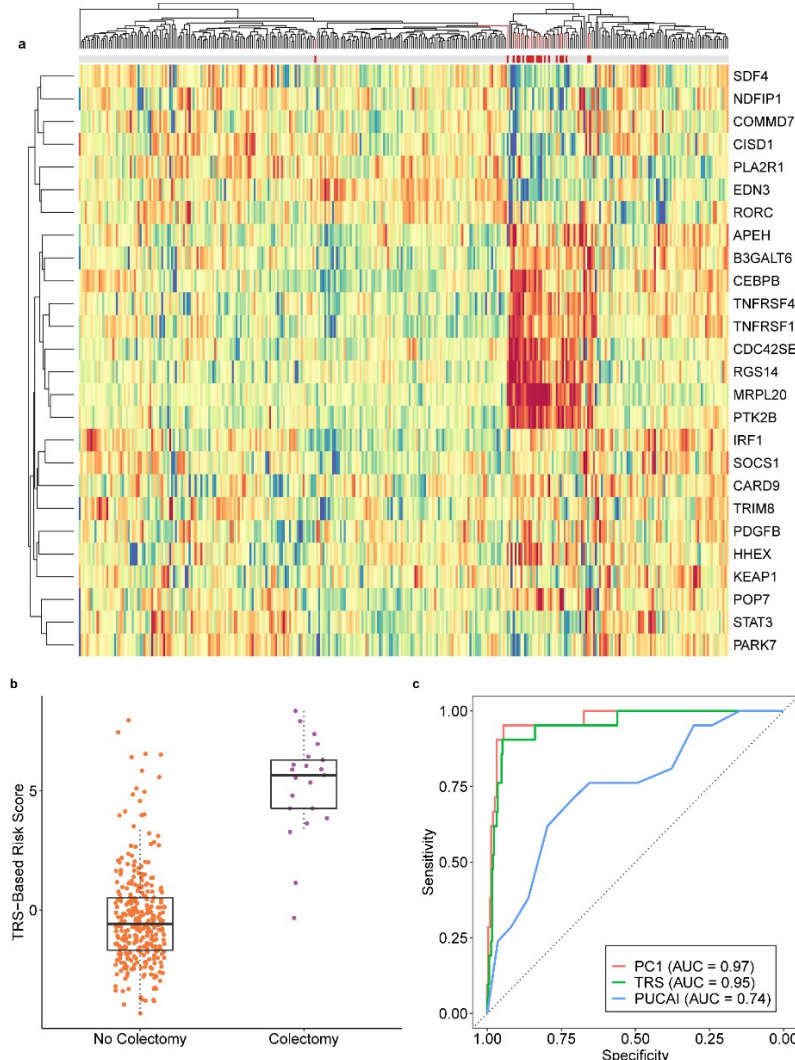
98  
99  
100 **Figure 2.** eQTL contrast between baseline and week 52 follow-up in the PROTECT study. (a) Comparison  
101 of effect sizes (betas) for the effect of the minor allele on gene expression. Blue eQTL were discovered  
102 at baseline, and magenta only at week 52. (b) Examples of nine genes with differential eQTL effects at  
103 the two timepoints showing observed transcript abundance as a function of genotype at baseline or  
104 week 52 follow-up. The bottom row are genes with eQTL only at follow-up. All boxplots indicate 1<sup>st</sup> and  
105 3<sup>rd</sup> quartile as box ends, with center median line and whiskers extending to farthest point within 1.5  
106 times the interquartile range. Note that many of the genes with large negative follow-up betas in panel  
107 (a) have relatively small minor allele frequencies, hence insufficient homozygous minor allele genotypes  
108 to plot. A full list of peak eQTL can be found in Table S3.

109 both time points, with the smaller number of eQTL at week 52 attributable to the smaller sample  
110 size. One quarter of the baseline eQTL are at least 2-fold greater than at week 52, and one third  
111 of the follow-up eQTL are at least 2-fold greater than at baseline. Clearly visible in Fig 2a are 33  
112 apparently week 52-specific effects that are more than 20-fold greater than at baseline, the  
113 majority with reduced expression of the minor allele. Examples of baseline and follow-up  
114 specific eQTL affecting a variety of gene functions in immunity and epithelial cell biology are  
115 shown in Fig. 2b. Some of the change in eQTL profiles is likely attributable to an increase in the  
116 proportion of epithelial relative to immune cells at week 52 (Fig. S3).

117 Next, we asked whether the intersection of GWAS, eQTL and differential expression could  
118 be used to generate a transcriptional risk score (TRS) for colectomy, analogous to the one we  
119 recently developed for prediction of risk of progression to complicated Crohn's disease<sup>11</sup>. The  
120 heatmap in Fig. 3a showing the abundance of 26 transcripts included in the TRS<sub>IBD</sub> derived with  
121 *coloc* overlap (26) of IBD GWAS and peripheral blood eQTL signals, indicates striking  
122 enrichment for elevated or reduced expression of a dozen transcripts in the baseline rectal  
123 biopsies of PROTECT patients destined for colectomy. The strongest clusters include *RGS14*,  
124 *MRPL20*, *PTK2B*, *TNFRSF4*, *TNFRSF18* and *CDC42SE2* up-regulation, and *CISDI*, *EDN3*,  
125 *RORC*, and *PLA2RI* down-regulation. PC1 of the entire set of 26 genes results in a TRS<sub>UC</sub> that  
126 discriminates colectomy from non-progressors at  $p=1\times 10^{-28}$  (Fig. 3b). A score above 3.24 has a  
127 sensitivity of 90% and specificity of 95% (Fig. 3c), generating a positive predictive value of  
128 55%, which is nine times the prevalence of the rate of progression in the study. Corresponding  
129 likelihood ratios for positive and negative prediction are 18 and 10 respectively. TRS<sub>UC</sub> also  
130 performs as well as the composite PC1 of all 2,500 differentially expressed genes.

131 We replicated these findings in an independent adult ulcerative colitis cohort from Mt

132 Sinai Medical School in New York<sup>27,28</sup>. PC1 of the rectal expression of 146 genes strongly  
133 correlated with the PROTECT PC1<sub>col</sub> signature highly significantly ( $p=0.0015$ ) distinguished 10



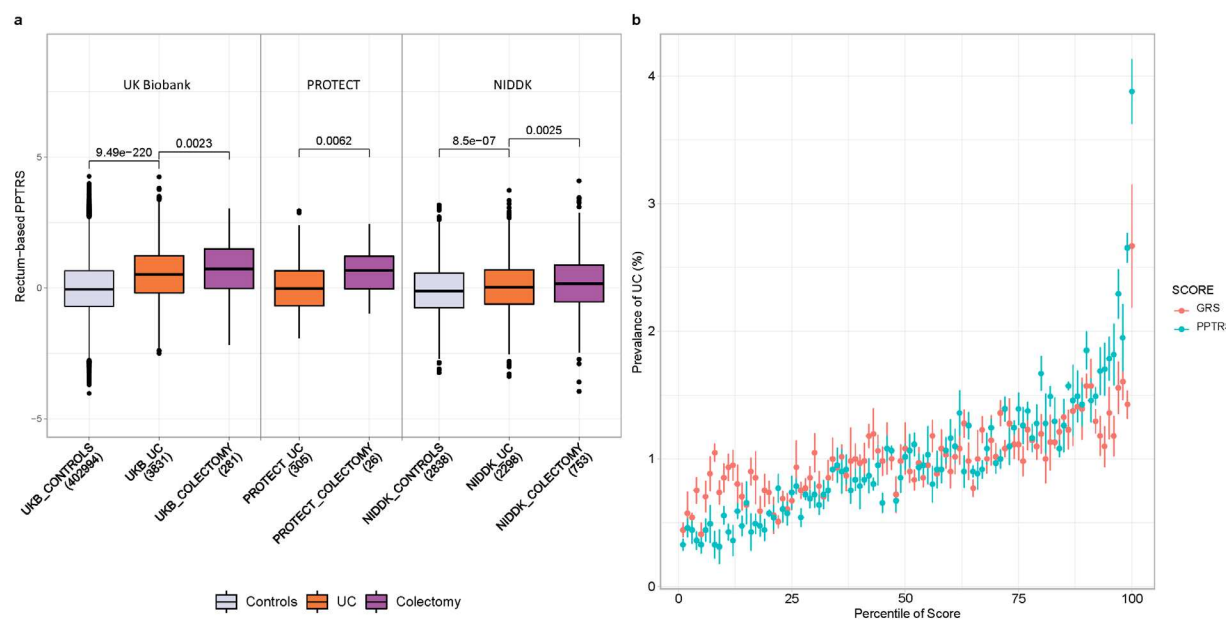
134  
135 **Figure 3.** Development of a Transcriptional Risk Score for Colectomy. (a) Heatmap of baseline rectal  
136 expression of 26 genes with evidence that the GWAS peak is the same as a blood eQTL (coloc H4 > 0.8),  
137 red high expression and blue low. The gray bar at the top indicates colectomy status, highlighting a  
138 cluster of patients for whom most of the genes are differentially expressed in the cases (red bars). (b)  
139 PC1 of the genes generates a TRS that is highly discriminatory between colectomy and non-colectomy at  
140 baseline;  $p=1\times 10^{-28}$ . Boxplots indicate 1<sup>st</sup> and 3<sup>rd</sup> quartile as box ends, with center median line and  
141 whiskers extending to farthest point within 1.5 times the interquartile range. (c) Receiver operating  
142 characteristic curve contrasting sensitivity and specificity for colectomy showing that both the TRS  
143 (green) and PC1 of all differentially expressed genes (red) have high accuracy (AUC > 0.95), compared  
144 with PUCAI, a commonly used clinical disease severity index.  
145

146 patients who have had colectomy from the remaining 201 (Fig. S4a), with the majority of genes  
147 differentially expressed in the same direction. Similarly, a TRS derived from the GWAS-  
148 associated 26 transcripts showed a strong trend toward differentiation of colectomy cases in the  
149 adult cohort (Fig. S4b), which was also significant ( $p=0.010$ ) after removal of two outliers  
150 characterized by aberrant expression of *CDC42SE2*, the only transcript in the list above which  
151 disagreed in direction of effect between the two studies.

152 Examination of the expression of colectomy-associated genes in a single cell RNAseq  
153 dataset obtained from rectal biopsies provides strong evidence that both epithelial and immune  
154 cells contribute to the risk of disease progression (Fig. S5). Most of the genes are strongly  
155 expressed in just one or two of the 22 identified cell types, seven of which are notable for an  
156 excess of colectomy associated genes: plasmacytoid dendritic cells, immunoregulatory T-cells,  
157 ILC1/3 innate immune cells, and inflammatory macrophages from the immune compartment,  
158 and fibroblasts, secretory epithelial, and endothelial cells from the gut itself. The correlated  
159 expression of these gene sets suggests that risk of colectomy may in part reflect abnormal  
160 relative abundance of these cell types. On the other hand, each of these cell types is also  
161 represented in the single cell profiles of the TRS genes, which were selected on the basis of joint  
162 eQTL and GWAS associations and hence are likely to be related to pathology through cis-  
163 regulatory effects. Prospective scRNAseq studies will likely reveal more insight into the cellular  
164 and genetic basis of the transcriptional risk of adverse disease progression.

165 Despite the strong contribution of trans-regulation to the TRSUC score, implied by the  
166 covariance of expression of the genes, the conjunction of GWAS and eQTL signals suggests that it  
167 may be possible to also predict disease progression from genotypes alone. To evaluate this, we  
168 performed a transcriptome-wide association study<sup>15,16</sup> using Dirichlet Process Regression (DPR)

169 implemented in TIGAR<sup>29</sup> to capture the effects of all polymorphisms within 1Mb of each  
170 transcript expressed in the PROTECT rectal biopsies, and then used the weights to predict gene  
171 expression in the White British subset of the UK Biobank<sup>21</sup>. We tested for differential predicted  
172 gene expression in 70% of the samples, and discovered ~800 genes either up- or down-regulated  
173 in ulcerative colitis cases relative to non-IBD controls. A predicted polygenic transcriptional risk  
174 score (PPTRS<sub>UC</sub>) was then derived as a weighted sum of the effect sizes of the minor alleles  
175 (which polarizes effects of alleles that increase or decrease expression in cases), and applied to the  
176 held-out 30% validation sample, as well as to the PROTECT genotypes. Figure 4a shows that the  
177 PPTRS efficiently discriminates UC cases from non-IBD controls in UK Biobank ( $p < 10^{-219}$ ), and  
178 remarkably that it also discriminates the colectomy cases in both UK Biobank and PROTECT  
179 ( $p = 0.002$  and 0.006



180  
181 **Figure 4.** Properties of a Predicted Polygenic Transcriptional Risk Score (PPTRS). (a) PPTRS developed  
182 from predicted gene expression in PROTECT used to identify predicted differentially expressed genes in  
183 the UK Biobank. The weighted sum of 820 predicted gene expression values clearly separates controls  
184 from ulcerative colitis cases in the UK Biobank, PROTECT and NIDDK studies, while colectomy cases have  
185 even more highly elevated scores. (b) Prevalence versus Percentile plots for a Polygenic Risk Score based  
186 on 6396 genotypes for UC (red) and the PPTRS (green), showing enhanced prevalence for the upper  
187 deciles of the PPTRS. Whiskers show standard error of mean from 5-fold validation.

188  
189 respectively, p-values computed using Kruskal-Wallis test in R). That is to say, as with the  
190 observed gene expression, colectomy cases are distinguished by a trend toward yet more extreme  
191 predicted gene expression. The same trend was replicated in a larger and completely independent  
192 NIDDK-IBDGC colectomy cohort<sup>30,31</sup>, consisting of 2838 non-IBD controls, 2298 cases  
193 diagnosed as UC, and 753 known colectomy cases. The rectum-based PPTRS in this cohort  
194 discriminates UC cases from non-IBD controls ( $p=8.5 \times 10^{-7}$ ) as well as UC from colectomy  
195 ( $p=0.0025$ ) (Fig. 4a).

196 Furthermore, PPTRS<sub>UC</sub> provides enhanced discrimination of cases and controls in the UK  
197 Biobank, as shown in the prevalence vs. risk score percentile plots in Fig. 4b. Whereas the top  
198 percentile has three-fold higher prevalence than the median using a PRS with 6,396 UC SNPs  
199 from summary statistics of the European UC GWAS meta-analysis<sup>32</sup> (pruned using PLINK at p-  
200 value  $< 0.001$ , LD  $r^2 > 0.5$ ), the top percentile of PPTRS<sub>UC</sub> is four-fold higher, and higher  
201 prevalence is inferred for the top 20% of the entire cohort. Negative predictive values are similar  
202 for both scores.

203 Although colectomy status was not incorporated into either the DPR-based prediction of  
204 gene expression or the computation of PPTRS<sub>UC</sub>, the fact that the prediction and testing datasets  
205 are both from PROTECT could confound the interpretation with an element of circularity. We  
206 thus used the GTEx study<sup>33</sup> transverse colon samples (n=368) to generate independent prediction  
207 models, which were then run through the same pipeline to generate a confirmatory PPTRS<sub>UC</sub>.  
208 Table 1 shows that this score was almost as good as the PROTECT-derived one in predicting  
209 colectomy in the UK Biobank, PROTECT and NIDDK studies ( $p=0.011$ ,  $p=0.007$  and  $p=0.006$   
210 respectively). Furthermore, neither cortex nor muscle-derived PPTRS from GTEx significantly  
211 predicts progression to colectomy (Table S1).

212 Our results highlight the potential of transcriptional profiling for prediction of colectomy  
213 in ulcerative colitis. Direct measurement of rectal biopsy RNA provides a highly discriminatory  
214 signature observed in almost all children who will need surgery, and which predicts the adverse  
215 outcome in up to half of all cases. This expression profile reverts to a healthier state regardless  
216 of immunological therapy within one year. Although much of the mis-expression is thus  
217 associated with disease status and due to trans-regulation<sup>34</sup>, we nevertheless show that prediction  
218 of gene expression from cis-linked SNPs is sufficient to generate a polygenic risk score that  
219 outperforms one based purely on GWAS associations. Our results are limited by the relatively  
220 small sample size of colectomies in the PROTECT study, which is nevertheless the largest  
221 treatment-naïve inception cohort to date. It is likely that more widespread sampling of this and  
222 other forms of inflammatory bowel disease will yield even more accurate predictors of disease  
223 progression, influencing personalized therapeutic decisions.

224 **METHODS**

225 **The PROTECT cohort**

226 428 participants aged 4 to 17 years were enrolled from 29 centers across North America into the  
227 PROTECT study upon clinical, histological, and endoscopic diagnosis of ulcerative colitis. Patients with  
228 disease extent beyond the rectum, a Pediatric Ulcerative Colitis Activity Index (PUCAI) score of  $\geq 10$ ,  
229 no prior therapy for colitis, and negative enteric bacterial stool culture were eligible to participate. All  
230 baseline assessments and sample collections were performed prior to the initiation of therapy. Initial  
231 treatment with mesalamine, oral corticosteroids, or intravenous corticosteroids was decided based on  
232 mild, moderate, or severe PUCAI. Following the baseline assessment, follow-up assessments were  
233 performed at 4, 12, and 52 weeks, with other therapeutic interventions administered based on guidelines  
234 for need additional medical therapy. Study parameters are described in further detail in Hyams et al (1).

235 **RNAseq data processing and differential expression analyses**

236 RNA was isolated from 340 rectal biopsies taken at baseline and 92 rectal biopsies taken at week  
237 52 follow-up. RNAseq was performed with the Lexogen QuantSeq 3' platform. Using FastQC, the  
238 single end 150 bp reads were trimmed and adapters were removed (2). Reads were mapped to human  
239 genome hg19 using hisat2, and the aligned reads were converted into read counts per gene with  
240 SAMtools and HTSeq in the default union mode (3),(4),(5). The raw read counts were normalized via  
241 trimmed mean of M-values normalization with the edgeR R package (6).

242 Expression of the sex-specific genes RPS4Y1, EIF1AY, DDX3Y, KDM5D, and XIST was used  
243 to validate the gender of each individual, resulting in the removal of two mismatches. Further  
244 adjustment and removal of batch effects was performed with surrogate variable analysis (SVA)  
245 combined with supervised normalization (SNM) (7),(8). Race, gender, initial treatment group, time of  
246 sampling, and week 52 colectomy status were modeled with the SVA R package, where initial treatment  
247 group, time of sampling, and week 52 colectomy status were protected variables, which resulted in the  
248 identification of 28 confounding factors. Of these, five variables significantly correlated with protected  
249 variables were preserved, while the remaining 23 were statistically removed with SNM. Two individuals  
250 that were outliers in a principal component analysis of total gene expression were removed.

251 Differential gene expression testing was performed based on colectomy status with the voom R  
252 package. Log fold change and Benjamini-Hochberg adjusted p-values were obtained for all genes. The  
253 first principal component of the top 150 genes differentially expressed at baseline between patients who  
254 required colectomy by week 52 follow-up (n= 21) and patients who did not (n= 310) formed the gene  
255 expression-based risk score for colectomy (PC1<sub>col</sub>). This score is moderately correlated (r=0.46) with  
256 PC1 of overall expression of genes differentiating UC cases and controls, reported by Haberman et al  
257 (2019) (reference 7 in main text).

258 Cross validation for PC1<sub>col</sub> was performed by randomizing colectomy status amongst individuals

259 prior to differential gene expression testing and calculation of  $PC1_{colRand}$ , as in the calculation for  $PC1_{col}$ .  
260 ANOVA was performed between randomized colectomy and non-colectomy individuals, with results  
261 from 1000 such tests reported in Fig. S1.

262 We compared expression of the genes comprising  $PC1_{col}$  at baseline and week 52 with Mayo  
263 score as a marker for mucosal healing (Fig. S2).  $PC1_{col}$  was calculated as previously described in the  
264 subset of individuals with baseline gene expression. Additionally, a restricted  $PC1_{col-wk52}$  was calculated  
265 by finding PC1 of the 150 genes used in the calculation of  $PC1_{col}$ , within the subset of individuals with  
266 week 52 gene expression. Change in PC1 score was simply calculated as the difference between  $PC1_{col}$   
267 and  $PC1_{col-wk52}$ . All p-values were generated with analysis of variance (ANOVA) tests.

268 Transcriptional Risk Scores (TRS), first introduced by Marigorta et al. (9) for discriminating  
269 IBD cases versus controls, capture the summation of polarized expression of genes incorporated based  
270 on both proximity to IBD GWAS hits and presence of eQTL in peripheral blood. We generated the TRS  
271 with four different strategies, all of which gave similar highly significant differentiation between  
272 colectomy and no colectomy samples. Model 1 was a GLM using the top 9 genes *RGS14*, *APEH*,  
273 *MRPL20*, *POP7*, *CDC42SE2*, *RORC*, *EDN3*, *PTK2B*, and *STAT3* that differentiate patients by  
274 colectomy status ( $p < 0.1$ ), essentially the sum of the z-scores weighted by their magnitude of  
275 differential expression. Model 2 was a GLM using the 10 genes discussed in the text due to strong co-  
276 regulation and association with colectomy. Models 3 and 4 were based on all 26 genes, generated with a  
277 weighted GLM or simple PC1 score, respectively. All four scores are highly correlated,  $r > 0.8$ ,  
278 indicating that they are capturing similar aspects of differential expression (Fig. S7). We report Model 4  
279 in the text. This TRS is highly correlated with  $PC1_{col}$  ( $r = 0.64$ ).

280 Relative proportions of epithelial and immune contributions to total rectal gene expression  
281 reported in Fig. S3 were evaluated by computing PC1 of the expression of 200 genes upregulated  
282 specifically in the total epithelial or immune components of the single cell gene expression dataset

283 reported by Smillie et al (10). We checked each PC to ensure that positive values associate with elevated  
284 expression of the respective genes, and compared the values at Baseline and Week 52.

285

286 **Replication of colectomy risk score and cell-type enrichment**

287 Surgical specimens from 210 ulcerative colitis patients undergoing bowel resection for IBD at  
288 Mount Sinai Health System and affiliated clinicians were recruited to be part of the Mount Sinai  
289 Crohn's and Colitis Registry (MSCCR) between December, 2013 and September, 2016 as described  
290 (11-13). The protocol required written informed consent that was approved by the Icahn School of  
291 Medicine at Mount Sinai Institutional Review Board (HSM#14-00210). Patients who were enrolled in  
292 the study were asked to provide blood and/or biopsies, which were collected during a colonoscopy  
293 planned for regular care. Clinical and demographic information was obtained through a questionnaire.  
294 Patients were treated with a range of medications, including corticosteroids, infliximab, azathioprine,  
295 and mesalamine. All macroscopically moderate-to-severely inflamed tissues were confirmed as active  
296 colitis by pathology examination provided by the Mount Sinai Hospital (MSH) Pathology Department.  
297 Freshly collected representative 0.5-cm-wide tissue fragments were isolated from surgical specimen  
298 samples, flash frozen, and stored at -80 °C.

299 RNA was isolated from frozen tissue using Qiagen QIAsymphony RNA Kit (cat.# 931636) and  
300 samples with RIN scores >7 were retained. One microgram of total RNA depleted of ribosomal RNA  
301 using the Ribozero kit (Illumina Cat # MRZG12324) was used for the preparation of sequencing  
302 libraries using RNA Tru Seq Kits (Illumina (Cat # RS-122-2001-48). These were sequenced on the  
303 Illumina HiSeq 2500 platform using 100 bp paired end protocol. Base calling from Images and  
304 fluorescence intensities of the reads was done in situ on the HiSeq 2500 computer using Illumina  
305 software, aiming for 70,000 paired end reads per sample. Short reads were mapped to the GRCh37/hg19  
306 assembly (UCSC Genome Browser) with 2-pasa STAR, and processed using RAPiD, which is a RNA-

307 seq analysis framework developed and maintained by the Technology Development group at the Icahn  
308 Institute for Genomics and Multi-scale Biology. Detailed quality control metrics were generated using  
309 the RNASEQC package. Raw count data was pre-filtered to keep genes with CPM>0.5 for at least 3% of  
310 the samples. After filtering, count data was normalized via the weighted trimmed mean of M-values and  
311 further variance stabilized using a logarithmic transformation. Normalized counts were further  
312 transformed into normally distributed expression values via the voom-transformation using a model that  
313 included technical covariates (processing batch, RIN, exonic rate and ribosomal RNA rate), while  
314 accounting for the intra-patient correlation across regions.

315 We repeated the transcriptional risk assessment analysis in this external dataset after  
316 normalization for gender, age, exonic RNA ratio, and rRNA level expression levels, using the *prcomp*  
317 function in R with the 150 genes from the PROTECT PC1<sub>col</sub>, or the 26 gene TRS. The R package  
318 ggplot2 was then used to plot the distribution of PC1 for patients who did (10 patients) or did not (201  
319 patients) have follow-up colectomies (Fig. S4). Additionally, we performed hierarchical clustering of  
320 single-cell gene expression data to identify cell types implicated by both the PC1 and TRS gene sets.  
321 Cell types enriched for PC1 genes included plasmacytoid dendritic cells, endothelial cells, group I innate  
322 lymphoid cells, fibroblasts, and macrophages.

323

## 324 **SNP data processing and eQTL studies**

325 The Affymetrix UK BioBank Axiom Array was used to perform genotyping of 424 individuals  
326 across 800,000 SNPs. Imputation was performed using IMPUTE2 software (14), after which quality  
327 control performed using PLINK was used to remove SNPs not in Hardy-Weinberg equilibrium at  $p <$   
328  $10^{-3}$ , SNPs with a minor allele frequency < 1%, or a rate of missing data across individuals > 5% (15).  
329 Approximately 7 million imputed SNPs passed these thresholds and were tested in the eQTL analysis.  
330 SNPs within 250 kb of the start and stop sites of a gene were considered to be *cis* to the gene and tested

331 for a potential eQTL association. Mapping was performed with the mixed linear modelling method in  
332 GEMMA, which tested a set of approximately 12 million SNP-gene pairs for associations at a common  
333 *p*-value threshold of  $1 \times 10^{-5}$  [(16)]. Two separate comparative analyses were performed, where the initial  
334 set of eQTL mapping was performed on all 330 baseline samples and 87 week 52 follow-up samples,  
335 and the secondary analysis was performed on 78 matched samples only, where the same individual was  
336 profiled at both time points. The initial full analysis yielded 91,774 significant SNP-gene associations at  
337 baseline and 19,371 associations at week 52 follow-up, and the secondary matched analysis yielded  
338 14,272 significant unique SNP-gene associations at baseline and 12,617 significant associations at week  
339 52 follow-up. These were further refined to 1,317, 218, 186, and 166 peak SNP to unique gene  
340 associations, respectively.

341 **Single cell sequence analysis of the lamina propria**

342 For the analyses reported in Supplementary Fig. S5, we analyzed a total of 34,157 cells from  
343 paired inflamed rectum ( $n = 4$ ) and uninflamed sigmoid colon ( $n = 5$ ) from 4 UC patients undergoing  
344 treatment at Mount Sinai Hospital. Resected tissue biopsies were collected in ice cold RPMI 1640  
345 (Corning Inc.) and processed within one hour after termination of the surgery. To limit biased  
346 enrichment of specific cell populations related to local variations in the intestinal micro-organization, we  
347 pooled twenty mucosal biopsies sampled all along the resected specimens using a biopsy forceps  
348 (EndoChoice). Epithelial cells were dissociated by incubating the biopsies in a dissociation medium  
349 (HBSS w/o  $\text{Ca}^{2+}$  or  $\text{Mg}^{2+}$  (Life Technologies) with HEPES 10mM (Life Technologies) and enriched  
350 with 5mM EDTA (Life Technologies)) at 37°C with 100 rpm agitation for two cycles of 15 min. After  
351 each cycle, the biopsies were vortexed vigorously for 30 seconds, and washed in complete RPMI media  
352 equilibrated at RT. They were transferred to digestion medium (HBSS with  $\text{Ca}^{2+}$   $\text{Mg}^{2+}$ , FCS 2%, DNase  
353 I 0.5mg/mL (Sigma-Aldrich) and collagenase IV 0.5mg/mL (Sigma-Aldrich)) for 40 min at 37°C with  
354 100 rpm agitation. After digestion, the cell suspension was filtered through a 70mm cell strainer, washed

355 in DBPS / 2% FCS / 1mM EDTA and spun down at 400 g for 10 min. After red blood cell lysis  
356 (BioLegend), dead cells were depleted using the dead cell depletion kit (Miltenyi Biotec, Germany),  
357 following manufacturer's recommendations. Viability of the final cell suspension was calculated using a  
358 Cellometer Auto 2000 (Nexcelom Biosciences) with AO/PI dye. The exclusion was routinely 70% or  
359 higher live cell rate.

360 Single cells were processed through the 10X Chromium platform using the Chromium Single  
361 Cell 3' Library and Gel Bead Kit v2 (10X Genomics, PN-120237) and the Chromium Single Cell A  
362 Chip Kit (10X Genomics, PN-120236) as per the manufacturer's protocol. In brief, 10,000 cells from  
363 single cell suspension were added to each lane of the 10X chip. The cells were partitioned into gel beads  
364 in emulsion in the Chromium instrument, in which cell lysis and bar-coded reverse transcription of RNA  
365 occurred, followed by amplification, fragmentation and 5' adaptor and sample index attachment.  
366 Libraries were sequenced on an Illumina NextSeq 500.

367 We aligned reads to the GRCh38 reference using the Cell Ranger v.2.1.0 Single-Cell Software  
368 Suite from 10X Genomics. The unfiltered raw matrices were imported into R Studio as a Seurat object  
369 (Seurat v3.0.1 (17)). Genes expressed in fewer than three cells in a sample were excluded, as were cells  
370 that expressed fewer than 500 genes and with UMI count less than 500 or greater than 60,000. We  
371 normalized by dividing the UMI count per gene by the total UMI count in the corresponding cell and  
372 log-transforming. The Seurat integrated model (17) was used to generate a combined ulcerative colitis  
373 model with cells from both inflamed and uninflamed samples retaining their group identity. We  
374 performed unsupervised clustering with shared nearest-neighbour graph-based clustering, using from 1  
375 to 15 principal components of the highly variable genes; the resolution parameter to determine the  
376 resulting number of clusters was also tuned accordingly. Cell types were assigned using known markers  
377 previously described for Crohns' disease (18). Visualization of relative abundance of specific genes in  
378 each cell type was performed using Seurat functions in conjunction with the ggplot2 (19).

379 **Gene expression imputation and prediction models**

380 We performed a transcriptome wide association study (TWAS) for association between the  
381 imputed *cis*-genetic component of gene expression with UC status. PROTECT (1) was used as the  
382 prediction study with both genetic and transcriptomic data from which to estimate *cis*-eQTL effects,  
383 which were then used to impute gene expression in the UK Biobank validation dataset. Subsequently,  
384 these predicted gene expression models were associated with UC status in the UK Biobank, and the  
385 significant ones were combined into a weighted Predicted Polygenic Transcriptional Risk Score  
386 (PPTRS) which was itself evaluated for association with UC, and secondarily with colectomy status, in  
387 PROTECT (1).

388 Before building the gene expression imputation models, we ensured that the prediction and  
389 validation studies were harmonized, such that the allele frequencies are correlated, by ensuring that the  
390 genotype matrix accounts correspond to the same allele in both datasets. Gene expression imputation  
391 models were built using a non-parametric Bayesian Dirichlet process regression (DPR) method (20,21)  
392 in TIGAR, which assumes a Dirichlet process prior on the effect size variance to estimate *cis*-eQTL  
393 effect sizes. A linear regression model was assumed for estimating *cis*-eQTL effect sizes:

394 
$$E_g = wX + \epsilon, \quad \epsilon \sim N(0, \sigma^2),$$

395 where  $E_g$  is the gene expression for a gene  $g$ ,  $X$  is the genotype matrix for all *cis*-genotypes (SNPs  
396 within 1MB of the flanking 5' and 3' ends),  $w$  is the vector of *cis*-eQTL effect sizes, and  $\epsilon$  is the error  
397 term assumed to be normally distributed with a mean of zero. The predicted (imputed) gene expression  
398 for gene  $g$  is computed as:

399 
$$E_{g\text{-pred}} = w^*X_{\text{new}},$$

400 where  $X_{\text{new}}$  is the *cis*-genotype matrix of the new genotype data or GWAS samples and  $E_{g\text{-pred}}$  is the  
401 predicted gene expression of the new data. The imputed gene expression is the *cis*-genetic component of  
402 the total gene expression derived from common *cis*-eQTLs and does not include the trans-component, or

403 environmental effects. TIGAR (20) has been shown to generate a 2 fold improvement in variance  
404 explained by multi-SNP models relative to just capturing the top cis-eQTLs (22), more than with similar  
405 imputation methods such as Predixcan and FUSION (23,24).

406 As prediction datasets, we initially utilized the PROTECT (1) cohort (rectal gene expression,  
407 n=331), confirmed with GTEx (27) transverse colon gene expression (n=368), and contrasted with  
408 GTEx muscle gene expression (n=706) and cortex gene expression (n=205) negative controls. Sigmoid  
409 colon has fewer samples, so was underpowered for these analyses, despite being closer to the rectum  
410 than transverse colon. A threshold of 5% imputation  $R^2$  was used to select genes with valid imputation  
411 models that were taken forward for testing in the UK Biobank and PROTECT (Fig. S6 shows boxplots  
412 of imputation  $R^2$  for all tissues and table S1 showing number of genes with imputation  $R^2 > 5\%$ ). Note  
413 that colectomy status was not used in the modeling of either the cis gene expression, nor generation of  
414 the PPTRS, so prediction of colectomy in PROTECT from the UK Biobank score should not be circular.  
415 However, use of the GTEx colon expression to generate the imputation models ensures that prediction,  
416 validation and testing are performed with three independent datasets (GTEx, UK Biobank, and  
417 PROTECT). Further, we also replicated these results on a larger and completely independent European  
418 subset of NIDDK IBD Genetics Consortium colectomy cohort, wherein the rectum- and colon-based  
419 PPTRS discriminated UC from colectomy, while the muscle- and cortex-based PPTRS were negative  
420 controls. Finally, we also generated the PPTRS on a subset of the UK Biobank, testing it on a held-out  
421 sample with similar results.

## 422 **Transcriptome wide association study and Predicted Polygenic Risk Score (PPTRS)**

423 For the validation dataset, the genotype data of UK Biobank was used, including 4112 Ulcerative  
424 Colitis cases and 402,994 Non-IBD Controls. The gene expression of 407,106 White British individuals  
425 was predicted using gene expression imputation models for genes with imputation  $R^2 > 5\%$ .  
426 Subsequently, a gene-based association test was performed by fitting a logistic regression model of the

427 predicted gene expression against UC case-control status to determine the weight (log odds ratio) and p-  
428 value for each gene.

429 We then built a TWAS-based polygenic risk score, which we call a Predicted Polygenic  
430 Transcriptional Risk Score (PPTRS). To assess the polygenic architecture of gene expression, we  
431 adopted a TWAS threshold for differentially expressed genes with TWAS *p*-value < 0.05. The PPTRS  
432 score was constructed by computing the weighted sum of the predicted gene expression, where the  
433 weights are the log of odds ratio from TWAS of UC in UK Biobank (25). This score, as expected,  
434 highly significantly differentiates cases and controls in the UK Biobank, and surprisingly also colectomy  
435 status. The same weights were then used to generate the PPTRS in PROTECT and NIDDK cohorts, and  
436 to evaluate association with colectomy status. This procedure was repeated with the GTEx eQTL  
437 models. The contrasting polygenic risk score derived from GWAS weights, GRS<sub>UC</sub>, was constructed  
438 using 6,396 UC SNPs from summary statistics of the European UC GWAS meta-analysis (26) (pruned  
439 using PLINK at *p*-value < 0.001, LD  $r^2$  > 0.5 in 10kb windows with a 5-SNP sliding step).

440 **NIDDK IBDGC Colectomy Cohort:** Samples were genotyped on the Illumina Global Screening Array  
441 at Feinstein Institute for Medical Research (Manhasset, NY) or at the Broad Institute (Boston, MA) as a  
442 part of the National Institute of Diabetes and Digestive and Kidney Diseases Inflammatory Bowel  
443 Disease Genetics Consortium (NIDDK-IBDGC). Following stringent pre-imputation QC metrics as  
444 previously described (28), genotypes were phased using Eagle2 (29) and imputation was performed  
445 using the Michigan Imputation Server and HRC r1.1 reference panel (30, 31). Variants with estimated  
446 imputation accuracy (Rsq) < 0.3 and minor allele frequency > 0.1% were excluded post-imputation,  
447 leaving 21.9 million variants available for analysis. Of the total 16,024 NIDDK IBDGC samples  
448 available post-QC, 14,659 were of European ancestry (defined as EUR Admixture proportion  $\geq 0.70$   
449 (32). These included 2838 non-IBD controls, 2298 UC diagnosed cases (1325 established non-  
450 colectomy), and 753 known colectomy cases. The predicted polygenic risk score for colectomy was

451 computed on these samples using predicted gene expression from the cis-eQTL weights calculated with  
452 DPR on the rectal gene expression from PROTECT, or alternatively colon, cortex and muscle gene  
453 expression from GTEX. The TWAS weights for inclusion in the PPTRS<sub>col</sub> from the UK Biobank are  
454 reported in Table S1, with code provided by S.N. to T.H.

455 **Ethics statement.** Each site's institutional review board approved the protocol and safety monitoring  
456 plan. Informed consent or assent was obtained for each participant.

457 **Data accessibility.** The RNAseq data for this study has been deposited to the NCBI GEO database,  
458 series "GSE150961". Data will be made completely openly accessible upon publication.

459

460 **Code availability statement.** No custom algorithms or software were utilized for this study, but the  
461 corresponding authors will gladly share parameters used upon request. Code for computation of the  
462 PPTRS is available at the following github link: <https://github.com/sn-GT/Measured-and-predicted-TRS.git>.

## ACKNOWLEDGEMENTS

Support for this study was provided by NIDDK through grants U01DK095745, R01DK119991, P01 DK046763, U01 DK062413], U24DK062429, and U01DK062422, as well as the Leona M. and Harry B. Helmsley Charitable Trust. The authors thank Urko Marigorta for his counsel in development of TRS, Frank Hamilton, MD, Dana Anderson, MD, James Everhart, PhD, Jose Serrano, MD, PhD, and Stephen James, MD from NIDDK for their guidance. This research has been conducted using the UK Biobank Resource under Application Number 17984 to GG. The authors thank PROTECT site investigators for patient recruitment and data gathering, to the research coordinators at the investigative sites for their tireless attention, and to the patients and families who graciously agreed to participate.

## REFERENCES

Alexander, D.H., Novembre, J., Lange, K. Fast model-based estimation of ancestry in unrelated individuals. *Genome Res.* **19**: 1655-1664 (2009).

Anders, S., Pyl, P.T., & Huber, W. HTSeq--a Python framework to work with high-throughput sequencing data. *Bioinformatics* **31**, 166-169 (2015).

Andrews S. FastQC: a quality control tool for high throughput sequence data.  
<https://www.bioinformatics.babraham.ac.uk/projects/fastqc/>.(2010)

Aragam, K.G., Dobbyn, A., Judy, R., Chaffin, M., Chaudhary, K., Hindy, G., et al. Limitations of contemporary guidelines for managing patients at high genetic risk of coronary artery disease. *J Am Coll Cardiol.* **75**, 2769-2780 (2020).

Bycroft, C. et al. The UK Biobank resource with deep phenotyping and genomic data. *Nature* **562**, 203-209 (2018).

Damask, A., Steg, P.G., Schwartz, G.G., Szarek, M., Hagström, E., et al; Regeneron Genetics Center and the ODYSSEY OUTCOMES Investigators. Patients with high genome-wide polygenic risk scores for coronary artery disease may receive greater clinical benefit from alirocumab treatment in the ODYSSEY OUTCOMES Trial. *Circulation* **141**, 624-636 (2020).

Das, S., et al. Next-generation genotype imputation service and methods. *Nat Genet.* **48**: 1284-1287. (2016).

Gamazon, E.R., et al. A gene-based association method for mapping traits using reference transcriptome data. *Nat Genet.* **47**, 1091-1098 (2015).

Giambartolomei, C. et al. A Bayesian framework for multiple trait colocalization from summary association statistics. *Bioinformatics* **34**, 2538-2545 (2018).

Graham, D.B., Xavier, R.J. Pathway paradigms revealed from the genetics of inflammatory bowel disease. *Nature* **578**, 527-539 (2020).

GTEX Consortium. Genetic effects on gene expression across human tissues. *Nature* **550**, 204–213 (2017).

Gusev, A. et al. Integrative approaches for large-scale transcriptome-wide association studies. *Nat. Genet* **48**, 245-252 (2016).

Gusev, A. et al. Transcriptome-wide association study of schizophrenia and chromatin activity yields mechanistic disease insights. *Nat Genet* **50**, 538-548 (2018).

Gibson, G. On the utilization of polygenic risk scores for therapeutic targeting. *PLoS Genet.* **15**, e1008060 (2019).

Haberman, Y. et al. Ulcerative colitis mucosal transcriptomes reveal mitochondriopathy and personalized mechanisms underlying disease severity and treatment response. *Nat Commun.* **10**, 38 (2019).

Haritunians, T., et al. Genetic predictors of medically refractory ulcerative colitis. *Inflamm Bowel Dis.* **16**, 1830-1840 (2010).

Howie, B.N., Donnelly, P., & Marchini, J. A flexible and accurate genotype imputation method for the next generation of genome-wide association studies. *PLoS Genet.* **5**, e1000529 (2009).

Hyams, J.S., et al. Factors associated with early outcomes following standardised therapy in children with ulcerative colitis (PROTECT): a multicentre inception cohort study. *Lancet Gastroenterol Hepatol.* **2**, 855-868 (2017).

Hyams, J.S. et al. Clinical and biological predictors of response to standardised paediatric colitis therapy (PROTECT): a multicentre inception cohort study. *Lancet* **393**, 1708-1720 (2019).

Kim, D., Langmead, B., Salzberg, S.L. HISAT: a fast spliced aligner with low memory requirements. *Nat Methods.* **12**, 357-360 (2015).

Kugathasan, S. et al. Prediction of complicated disease course for children newly diagnosed with Crohn's disease: a multicentre inception cohort study. *Lancet* **389**, 1710-1718 (2017).

Lambert, S.A., Abraham, G., & Inouye, M. Towards clinical utility of polygenic risk scores. *Hum Mol Genet.* **28(R2)**, R133-R142 (2019).

Lee, J.C., Biasci, D., Roberts, R., Gearry, R.B., Mansfield, J.C., et al. Genome-wide association study identifies distinct genetic contributions to prognosis and susceptibility in Crohn's disease. *Nat Genet.* **49**, 262-268 (2017).

Leek, J.T., Johnson, W.E., Parker, H.S., Jaffe, A.E., & Storey, J.D. The sva package for removing batch effects and other unwanted variation in high-throughput experiments. *Bioinformatics* **28**, 882-883 (2012).

Leijonmarck, C.E., Persson, P.G. & Hellers, G. Factors affecting colectomy rate in ulcerative colitis: an epidemiologic study. *Gut* **31**, 329-333 (1990).

Lewis, C.M. & Vassos, E. Polygenic risk scores: from research tools to clinical instruments. *Genome Med.* **12**, 44 (2020).

Li, H., et al. The Sequence Alignment/Map format and SAMtools. *Bioinformatics* **25**, 2078-9 (2009).

Liu, J.Z. et al. Association analysis identify 38 susceptibility loci for inflammatory bowel disease and highlight shared genetic risk across populations. *Nat Genet* **47**, 979-986 (2015).

Lloyd-Jones, L.R. et al. The genetic architecture of gene expression in peripheral blood. *Am J Hum Genet.* **100**, 228-237 (2017).

Loh, P-R., et al. Reference-based phasing using the Haplotype Reference Consortium panel. *Nat Genet.* **48**: 1443-1448 (2016).

McCarthy, S., et al. A reference panel of 64,976 haplotypes for genotype imputation. *Nat Genet.* **48**: 1279-1283 (2016).

Marigorta, U.M. et al. Transcriptional risk scores link GWAS to eQTLs and predict complications in Crohn's disease. *Nat Genet.* **49**, 1517-1521 (2017).

Martin, J.C., Chang, C., Boschetti, G., Ungaro, R., Giri, M., et al. Single-cell analysis of Crohn's disease lesions identifies a pathogenic cellular module associated with resistance to anti-TNF therapy. *Cell* **178**, 1493-1508.e20 (2019).

Mecham, B.H., Nelson, P.S., & Storey, J.D. Supervised normalization of microarrays. *Bioinformatics* **26**, 1308-1315 (2010).

Nagpal, S. et al. TIGAR: An improved Bayesian tool for transcriptomic data imputation enhances gene mapping of complex traits. *Am J Hum Genet.* **105**, 258-266 (2019).

Naito, T., Botwin, G.J., Haritunians, T., Li, D., Yang, S., Khrom, M., Braun, J., NIDDK IBD Genetics Consortium, Abbou, L., Mengesha, E., Stevens, C., Masamune, A., Daly, M., McGovern, D.P.B. Prevalence and effect of genetic risk of thromboembolic disease in inflammatory bowel disease. *Gastroenterology* in press: S0016-5085(20)35276-8 (2020).

Natarajan P, Young R, Stitziel NO, Padmanabhan S, Baber U, Mehran R, et al. Polygenic risk score identifies subgroup with higher burden of atherosclerosis and greater relative benefit from statin therapy in the primary prevention setting. *Circulation* **135**, 2091-2101 (2017).

Ndungu, A., Payne, A., Torres, J.M., van de Bunt, M. & McCarthy, M.I. A Multi-tissue Transcriptome analysis of human metabolites guides interpretability of associations based on multi-SNP models for gene expression. *Am J Hum Genet* **106**, 188-201 (2020).

Parikh, K., Antanaviciute, A., Fawkner-Corbett, D., Jagielowicz, M., Aulicino A., et al. Colonic epithelial cell diversity in health and inflammatory bowel disease. *Nature* **567**, 49-55 (2019).

Peters, L.A. et al. A functional genomics predictive network model identifies regulators of inflammatory bowel disease. *Nat Genet* **49**, 1437-1449 (2017).

Purcell, S., et al. PLINK: a tool set for whole-genome association and population-based linkage

analyses. *Am J Hum Genet.* **81**, 559-575 (2007).

Robinson, M.D., McCarthy, D.J., & Smyth, G.K. edgeR: a Bioconductor package for differential expression analysis of digital gene expression data. *Bioinformatics* **26**, 139-140 (2010).

Sandborn, W.J. et al. Colectomy rate comparison after treatment of ulcerative colitis with placebo or Infliximab. *Gastroenterology* **137**, 1250-1260 (2009).

Schroeder, K.W., Tremaine, W.J. & Ilstrup, D.M. Coated oral 5-aminosalicylic acid therapy for mildly to moderately active ulcerative colitis. A randomized study. *N Engl J Med* **317**, 1625-1629 (1987).

Stuart, T, et al. Comprehensive integration of single-cell data. *Cell* **177**, 1888-1902.e21 (2019).

Suarez-Farinás, M., et al. Disease demarcation in ulcerative colitis is associated with different patterns of gene expression. *J Crohn's Colitis* **12**(Suppl 1), DOP012 (2018).

Suárez-Fariñas, M., et al. Intestinal inflammation modulates the expression of *ACE2* and *TPRSS2* and potentially overlaps with the pathogenesis of SARS-CoV-2 related disease. *bioRxiv* doi: <https://doi.org/10.1101/2020.05.21.109124>. *Gastroenterology*, in press. (2020)

Smillie, C.S., Biton, M., Ordovas-Montanes, J., Sullivan, K.M., Burgin, G., et al. Intra- and inter-cellular rewiring of the human colon during ulcerative colitis. *Cell* **178**, 714-730.e22 (2019).

Subramanian, A. et al. Gene set enrichment analysis: a knowledge-based approach for interpreting genome-wide expression profiles. *Proc Natl Acad Sci (USA)* **102**, 15545-15550 (2005).

Turner, D. et al. Appraisal of the pediatric ulcerative colitis activity index (PUCAI). *Inflamm Bowel Dis.* **15**, 1218-1223 (2009).

Ungaro, R., Mehandru, S., Allen, P.B., Peyrin-Biroulet, L. &and Colombel, J-F. Ulcerative colitis. *Lancet* **389**, 1756-1770 (2017).

Uzzan, M., et al. Mapping of B cell landscape in ulcerative colitis lesions reveals a pathogenic response that associates with treatment resistance and disease complications. *Nat. Medicine* 2020; Under second revision.

Wainberg, W. et al. Opportunities and challenges for transcriptome-wide association studies. *Nat Genet.* **51**, 512-599 (2019).

Wickham, H. *ggplot2: elegant graphics for data analysis*. 2nd ed. Cham: Springer (2016)

Zeng, P. & Zhou, X. Non-parametric genetic prediction of complex traits with latent Dirichlet process regression models. *Nat Commun* **8**, 456 (2017).

Zhou, X., & Stephens, M. Genome-wide efficient mixed-model analysis for association studies. *Nat Genet.* **44**, 821-824 (2012).

## Affiliations

### **1. Georgia Institute of Technology, Atlanta, 30332, GA, USA**

Angela Mo, Sini Nagpal, Dalia Arafat, and Greg Gibson

### **2. Charles Bronfman Institute of Personalized Medicine, Icahn School of Medicine at Mt Sinai, New York City, 10029, NY, USA**

Kyle Gettler, Mamta Giri, Nai-Yun Hsu, Ling-Shiang Chuang, Judy Cho

### **3. F. Widjaja Foundation Inflammatory Bowel and Immunobiology Research Institute, Cedars-Sinai Medical Center, Los Angeles, 90048, CA, USA**

Talin Haritunians, Emebet Mengesha, Dermot P. McGovern

### **4. Cincinnati Children's Hospital Medical Center, and the University of Cincinnati College of Medicine, 45229, Cincinnati, OH, USA**

Yael Haberman, Rebekah Karns, Bruce J. Aronow & Lee A. Denson

### **5. Sheba Medical Center, Tel Hashomer, Tel Aviv University, Tel Aviv, 5265601, Israel**

Yael Haberman

### **6. Emory University, Atlanta, 30322, GA, USA**

Jarod Prince, Cary G. Sauer and Subra Kugathasan

### **7. Icahn Institute for Data Science and Genomic Technology, and Department of Population Health Science and Policy, Mt Sinai School of Medicine, New York City, 10029, NY, USA**

Mayte Suarez-Farinias, Carmen Argmann, Andrew Kasarskis,

### **8. University of North Carolina, Chapel Hill, 27516, NC, USA**

Nathan Gotman

### **9. Harvard—Children's Hospital Boston, Boston, 02115, MA, USA**

Paul A. Rufo

### **10. Women & Children's Hospital of Buffalo WCHOB, Buffalo, 14222, NY, USA**

Susan S. Baker

### **11. Cohen Children's Medical Center of New York, 11040, New Hyde Park, NY, USA**

James Markowitz

### **12. Riley Hospital for Children, Indianapolis, 46202, IN, USA**

Marian D. Pfefferkorn

### **13. Goryeb Children's Hospital—Atlantic Health, Morristown, 07960, NJ, USA**

Joel R. Rosh

**14. Nationwide Children's Hospital, Columbus, 43205, OH, USA**

Brendan M. Boyle

**15. Children's Hospital of East Ontario, Ottawa, Ontario, K1P 1J1, Canada**

David R. Mack

**16. The Children's Hospital of Philadelphia, Philadelphia, 19104, PA, USA**

Robert N. Baldassano

**17. Children's Hospital of Pittsburgh of UPMC, Pittsburgh, 15224, PA, USA**

Sapana Shah

**18. Columbia University, Department of Pediatrics, New York City, 10032, NY, USA**

Neal S. LeLeiko

**19. University of California at San Francisco, San Francisco, 94143, CA, USA**

Melvin B. Heyman

**20. Hospital for Sick Children, Toronto, M5G 1X8, Canada**

Anne M. Griffiths & Thomas D. Walters

**21. UT Southwestern, Dallas, 75390, TX, USA**

Ashish S. Patel

**22. Medical College of Wisconsin, Milwaukee, 53226, WI, USA**

Joshua D. Noe

**23. RTI International, Research Triangle Park, 27709, NC, USA**

Sonia Davis Thomas

**24. Connecticut Children's Medical Center, Hartford, 06106, CT, USA**

Jeffrey S. Hyams

**Table 1. Summary of PPTRS results**

Summary of PPTRS Results								
Training data for transcriptomic imputation	Reference transcriptome	Number of genes with gene expression imputation $R^2 > 5\%$	Number of genes with TWAS $P < 0.05$ in UKBB UC vs Cont association & used in PPTRS	PPTRS P-values				
				UK Biobank		PROTECT	NIDDK IBDGC	
				UC vs Controls	UC vs COLECTOMY	UC vs COLECTOMY	UC vs Controls	UC vs COLECTOMY
PROTECT	Rectum (n=331)	9392	820	2.94E-210**	0.0023*	0.0062*	8.5e-07**	0.0025*
GTEX	Colon - Transverse (n=368)	13410	1097	4.71E-170**	0.011*	0.0073*	7.83e-12**	0.006*
Negative Controls for UC vs Colectomy								
GTEX	Muscle (n=706)	9963	777	1.57e-181**	0.089	0.220	1.69e-19**	0.290
GTEX	Cortex (n=205)	13486	1075	5.54e-215**	0.071	0.065	3.73e-19**	0.110

**Supplementary Table 1**

Supplementary Table S1.xlsx: Summary of PPTRS results including list of genes in each tissue.

**Supplementary Table 2**

Supplementary Table S2.xlsx: Summary of GSEA pathway results.

**Supplementary Table 3**

Supplementary Table S3.xlsx: Summary of peak eQTL identified in baseline and week 52 cohorts.

## Supplementary Figure 1

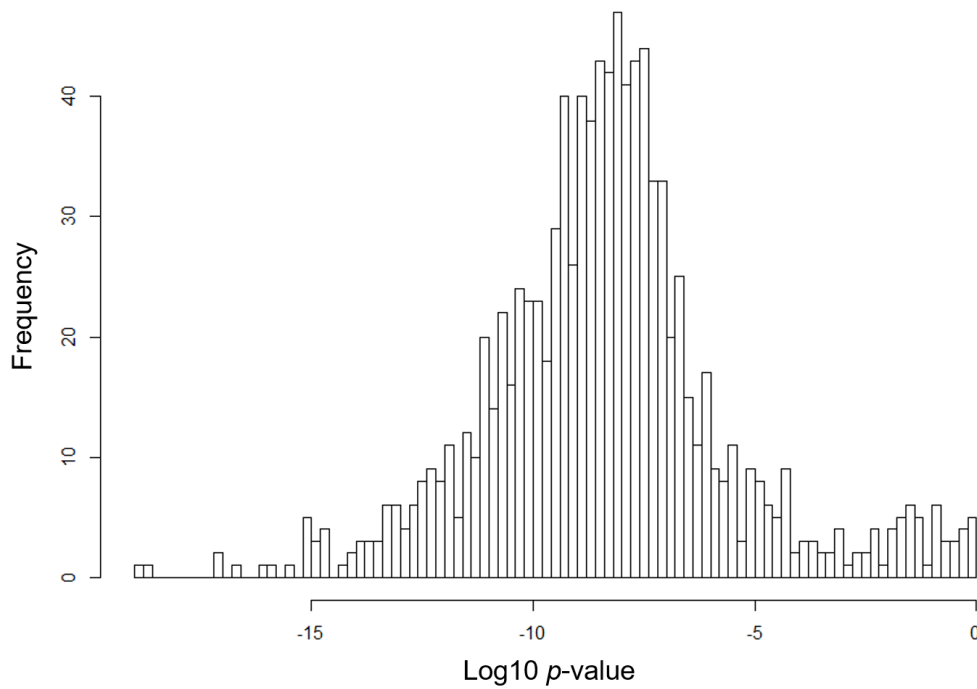


**Figure S1.** Permutation of  $\text{PC1}_{\text{col}}$ . Colectomy status was randomized prior to differential expression testing and calculation of  $\text{PC1}_{\text{colRand}}$ . Histogram shows frequency of  $\log_{10}$  p-value for ANOVA test of  $\text{PC1}_{\text{colRand}}$  between randomized colectomy and non-colectomy individuals in 1000 trials. Scores tend to be significant because the PC1 is derived from transcripts that are generally significant by chance in the permuted data. However, the significance is orders of magnitude less than that derived from the actual colectomy data:  $\text{PC1}_{\text{col}}$  true p =  $2 \times 10^{-45}$ .

## Supplementary Figure 2

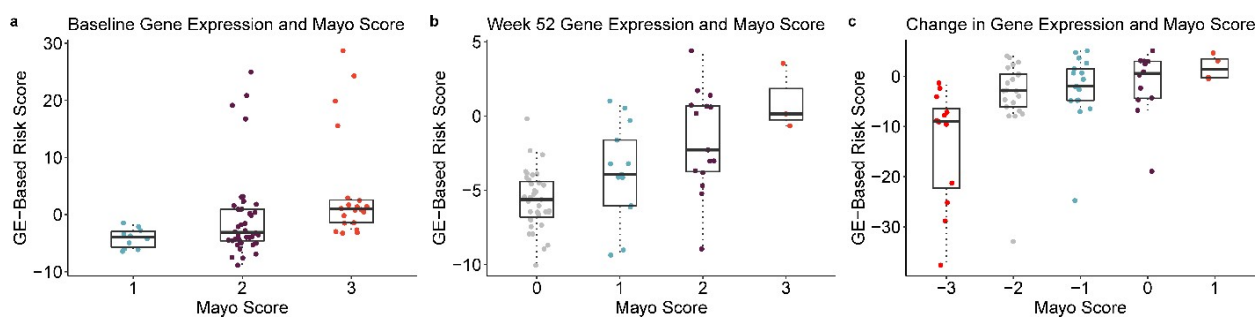


**Figure S2.** Associations between  $\text{PC1}_{\text{col}}$  and Mayo score. All boxplots indicate 1<sup>st</sup> and 3<sup>rd</sup> quartile as box ends, with center median line and whiskers extending to farthest point within 1.5 times the interquartile range. (a)  $\text{PC1}_{\text{col}}$  calculated on baseline gene expression with baseline Mayo score; p=0.004. (b)  $\text{PC1}_{\text{col}}$  calculated on week 52 gene expression with week 52 Mayo score; p=8.73×10<sup>-8</sup>. (c) Change in  $\text{PC1}_{\text{col}}$  and Mayo score from baseline to week 52; p=4×10<sup>-4</sup>.

### Supplementary Figure 3

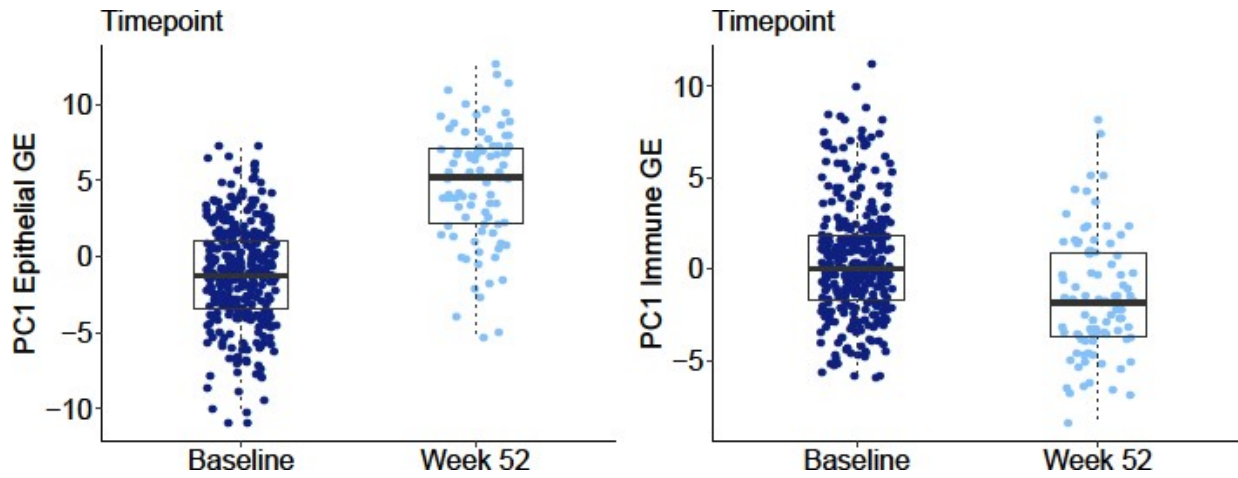


**Figure S3.** Switch in proportions of epithelial and immune components of rectal gene expression between baseline and week 52 follow-up. All boxplots indicate 1<sup>st</sup> and 3<sup>rd</sup> quartile as box ends, with center median line and whiskers extending to farthest point within 1.5 times the interquartile range. First principal components of 200 genes differentially expressed between the two tissue compartments in [Supplement ref. 27] were calculated and polarized such that PC1 reflects elevated expression of the genes. These results imply that immune activity is suppressed at week 52, and epithelial activity relatively elevated.

## Supplementary Figure 4

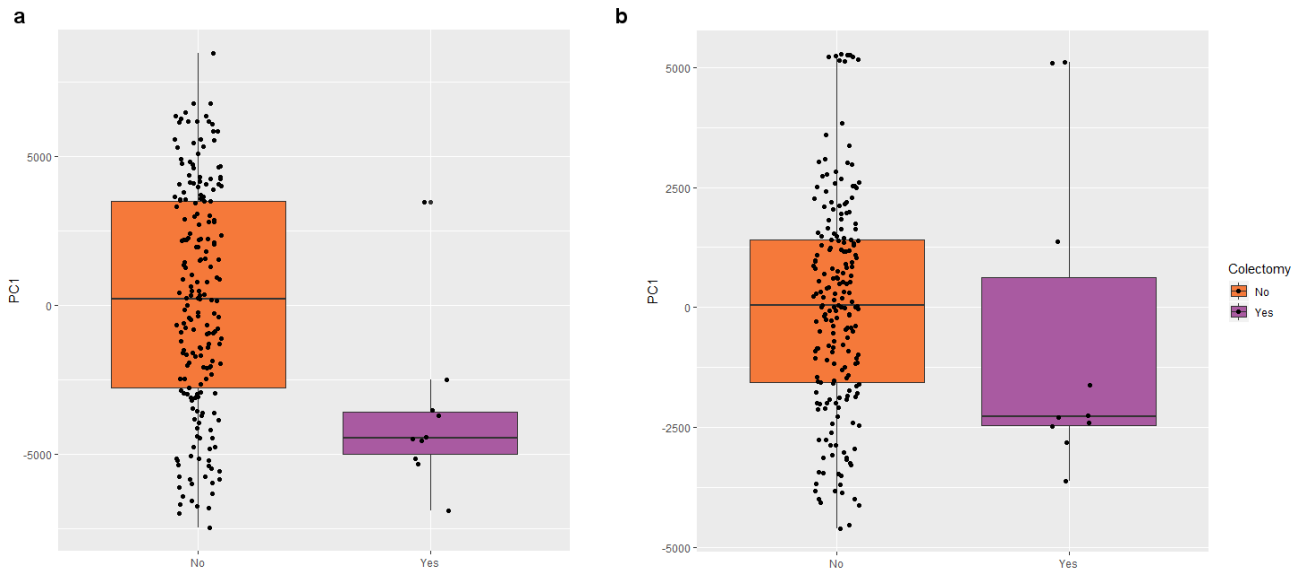
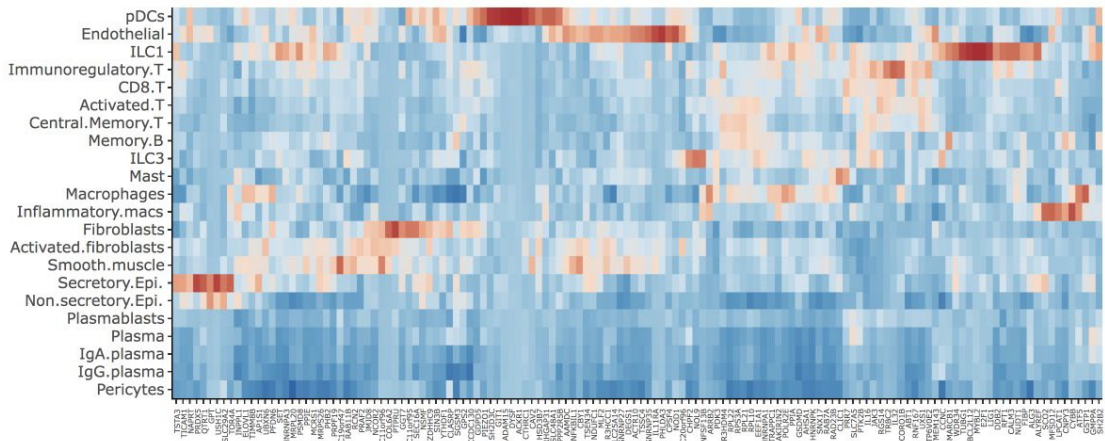


**Figure S4.** Replication of transcriptional risk prediction in the Mt Sinai cohort. All boxplots indicate 1<sup>st</sup> and 3<sup>rd</sup> quartile as box ends, with center median line and whiskers extending to farthest point within 1.5 times the interquartile range. (a) PC1 of colectomy-associated genes in Mt Sinai significantly differentiates colectomy (purple) from non-colectomy (orange). (b) TRS<sub>UC</sub> developed from IBD GWAS-associated genes also predicts progression to colectomy in the Mt Sinai cohort. Two outlier samples reduce the significance, which is  $p=0.01$  for the remaining samples.

## Supplementary Figure 5

a.



b.

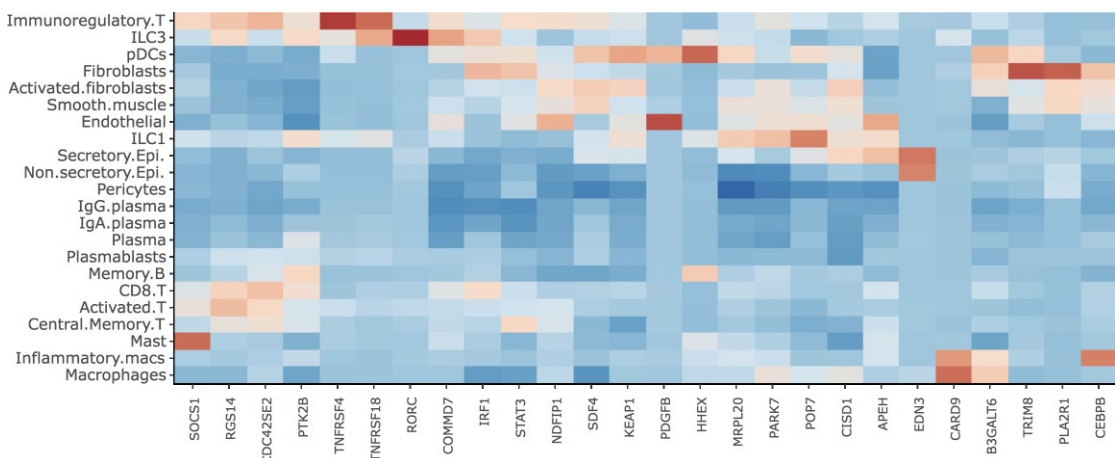


**Figure S5.** Cell-type specific expression of colectomy-associated genes. (a) Heat map showing up-regulation (red) of each gene contributing to PC1 in a rectal scRNASeq dataset. Dozens of genes are enriched in seven cell-types. (b) Similar analysis but for the TRS<sub>UC</sub> genes. Note the similarity of the cell-types showing enrichment, and the absence of B-cell or plasma cell signals in both.

## Supplementary Figure 6

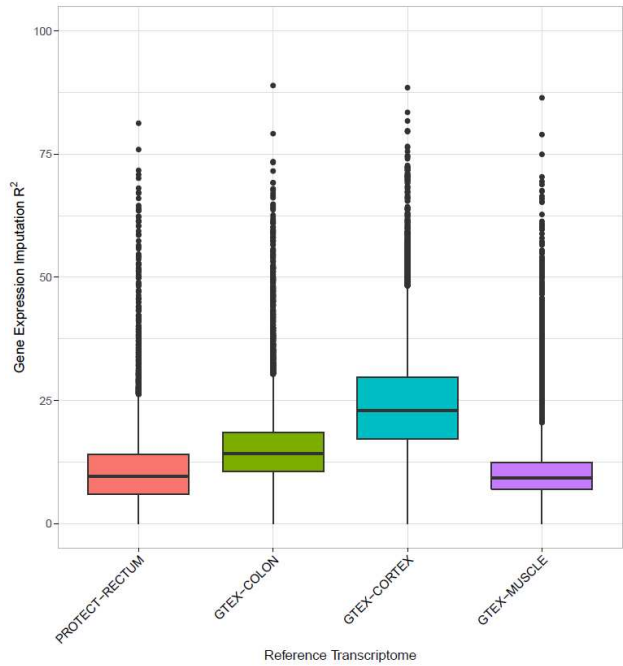


**Figure S6.** Distribution of  $R^2$  values for gene expression prediction models from each tissue. Each boxplot shows the median value of the variance in gene expression explained by DPR prediction with upper and lower hinge representing first and third quartiles (25<sup>th</sup> and 75<sup>th</sup> percentiles). The upper and lower whiskers extends no further than  $1.5 \times \text{IQR}$  (inter-quartile range) and data points beyond the end of whiskers are outliers.

## Supplementary Figure 7

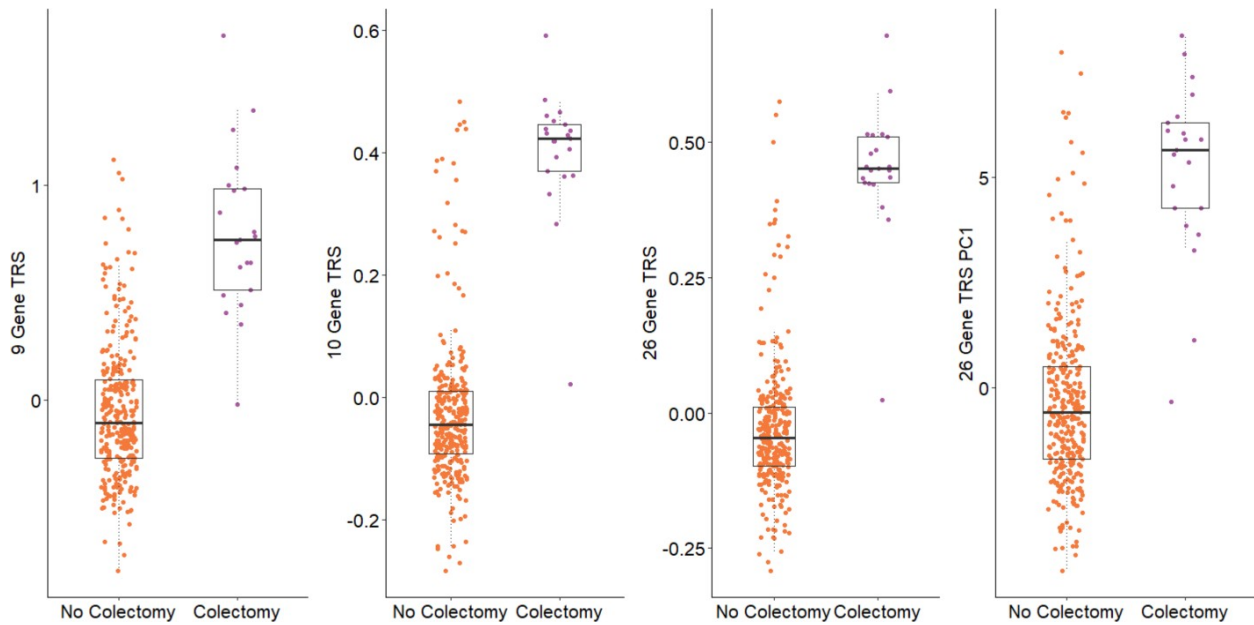


**Figure S7.** Comparison of TRS generated with different subsets of genes. Each plot shows the computed TRS for each individual who did or did not require colectomy during the study period. All boxplots indicate 1<sup>st</sup> and 3<sup>rd</sup> quartile as box ends, with center median line and whiskers extending to farthest point within 1.5 times the interquartile range. (a) 9 gene TRS for genes significantly differentiated by status at  $p<0.1$ ;  $p=2\times10^{-25}$ . (b) 10 gene TRS for genes highlighted in the text as the major clusters of up- and down-regulated in colectomy;  $p=8\times10^{-43}$ . (c) 26 gene TRS as sum of z-scores weighted by the magnitude of differential expression;  $p=9\times10^{-49}$ . (d) TRS computed simply as PC1 of the 26 genes;  $p=1\times10^{-28}$ .